CRYSTAL GROWTH & DESIGN

Article

pubs.acs.org/crystal

Supramolecular Complexes of Sulfadiazine and Pyridines: Reconfigurable Exteriors and Chameleon-like Behavior of Tautomers at the Co-Crystal−Salt Boundary

Published as part of the Crystal Growth & Design virtual special issue In Honor of Prof. G. R. Desiraju

Elizabeth Elacqua,[†] Dejan-Krešimir Bučar,[†] Rodger F. Henry,[‡] Geoff G. Z. Zhang,*[,§] and Leonard R. MacGillivray*[,†]

[†]Department of Chemistry, University of Iowa, Iowa City, Iowa 52242, United States

[‡]Structural Chemistry, Global Pharmaceutical R&D, Abbott Laboratories, North Chicago, Illinois 60046, United States

[§]Materials Science, Global Pharmaceutical R&D, Abbott Laboratories, 200 Abbott Park Road, Abbott Park, Illinois 60046, United States

Supporting Information

ABSTRACT: We apply crystal engineering principles to prepare organic co-crystals and salts of sulfadiazine and pyridines. Pyridines are molecular building blocks utilized in crystal engineering that can disrupt the hydrogen bonded (amidine) N−H···N (pyrimidine) dimer within the parent sulfa drug (SD) crystals, while providing access to both co-crystals and salts. We have synthesized four co-crystals and three salts of sulfadiazine involving *N*,*N*-dimethyl-4-aminopyridine, 4-aminopyridine, 4-picoline, 4,4′-bipyridine, (*E*)-1,2-bis(4-pyridyl)ethylene, 1,2-bis(4-pyridyl)acetylene, and 4-(pyridin-4-yl)piperazine. Single-crystal X-ray analyses reveal three hydrogen-bond motifs, namely, dyads, rings, and chains based involving either (amidine/aniline) N−H···N (pyridine/pyrimidine), (pyridinium) $^{+}$N−H···N^{-} (amidide), (aniline/piperazine) N−H···O_2S (sulfoxide) interactions, or a combination thereof. The hydrogen-bond motifs are assigned as $D_1^1(2)$, $R_2^2(8)$, $R_2^2(20)$, $C_2^2(17)$, and $C_2^2(13)$ graph sets. An analysis of the Cambridge Structural Database (CSD) reveals that the S−N bond length is generally shorter in complexes based on an anionic SD, which is consistent with the sulfonamide possessing greater S═N character. From an analysis of SD-based structures involving our work and the CSD, we present a heretofore not discussed role of tautomers at the co-crystal−salt boundary. Specifically, the ability of tautomeric forms of SDs to display reconfigurable exteriors, and thereby act as chameleons, enables SDs to accommodate different co-formers by assuming different geometries and adopting different regions along the co-crystal−salt boundary.

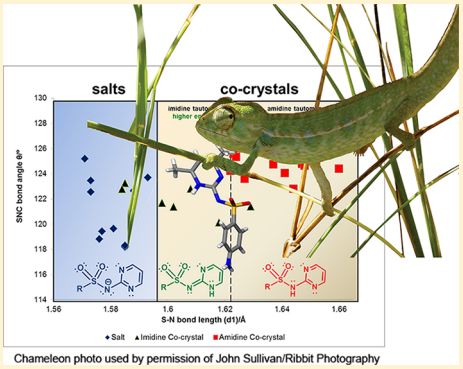

Chameleon photo used by permission of John Sullivan/Ribbit Photography

INTRODUCTION

The ability to design multicomponent pharmaceutical crystalline materials is based largely on the use of reliable noncovalent interactions (e.g., hydrogen bonds, $\pi-\pi$ forces) between constituent components in the form of supramolecular synthons.[1] Synthon hierarchies[2] are achieved *via* extensive co-crystallization[3] studies of model pharmaceutical agents (PAs) with structurally analogous co-formers that can participate in specific hydrogen-bonding motifs. Caffeine[4] and carbamazepine (CBZ)[5] have been utilized as prototypical PAs to identify robust supramolecular synthons based on (amide) N−H···O═C (amide), (acid) O−H···O═C (amide), (acid) O−H···N (imidazole), and (phenol) O−H···O═C (urea) forces in co-crystals. Whereas the number of supramolecular synthons employed in crystal engineering continues to rapidly grow, there remains a need to continue investigating roles of organic functionalities that can affect processes of drug discovery and development.[6]

Despite a widespread presence in drugs and related pharmaceutical compounds, sulfoxides ($-SO_2$) are less studied in the context of crystal engineering.[7] Moreover, whereas a search of the Cambridge Structural Database (CSD) reveals that supramolecular synthons exhibit a tendency to compete in solid-state materials based on sulfonates,[8] less is known about how sulfa drugs (SDs)[9] behave in organic co-crystals and salts.[10] SDs are the original class of PAs with an aniline ring covalently attached to a sulfonamide (SO_2NHR) moiety as a structural core. SDs were the first compounds used to systematically treat and prevent bacterial and microbial infections, while thriving on synergistic effects stemming from a mixture of at least two PAs (e.g., co-trimoxazole: 1:5 mix of sulfamethoxazole and trimethoprim).[11] Owing to a drive by the field of pharmaceutics to investigate how intermolecular

Received: November 28, 2012
Published: December 5, 2012

interactions between drug molecules dictate therapeutic efficacy, novel solid forms of SDs merit consideration to develop pharmaceutical co-crystals.[12]

To efficiently generate multicomponent pharmaceutical solids, it is of fundamental importance to analyze a target PA, evaluate how the molecule interacts with itself in the solid state, and identify dominant supramolecular synthons. In this context, the SD sulfadiazine (SDZ) possesses both hydrogen-bond-donor and -acceptor groups that can be targeted to form multiple synthons (Scheme 1a). SDZ, in the pure form, self-

Scheme 1. Schematic of (a) SDZ and (b) Self-Assembly in the Solid State Involving Primary (Sulfonamide) N−H···N (Pyrimidine) and Secondary (Aniline) N−H···O_2S (Sulfoxide) Forces

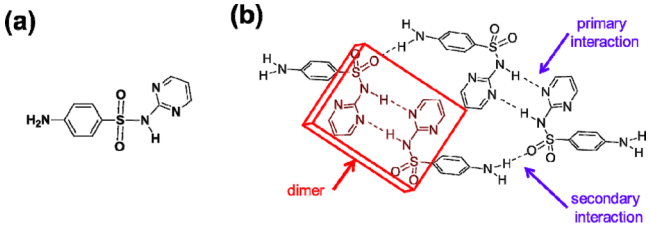

assembles *via* a complementary (amidine) N−H···N (pyrimidine) synthon, generating dimers that interact *via* secondary (aniline) N−H···O_2S (sulfoxide) forces (Scheme 1b).[13] Such two-point interactions are well-documented in the field of molecular recognition (e.g., amide/acid recognition).[14] To date, multicomponent complexes of SDZ have not been reported, which is likely owing to a marked low solubility in common organic solvents relative to other SDs. To achieve multicomponent solids based on SDZ, the use of a co-former with appreciably strong hydrogen-bond-donors and/or -acceptors able to compete with the hydrogen-bond-accepting pyrimidine functionality would be preferred to help limit dimer formation.[15]

Herein, we report the design and construction of multicomponent crystalline solids of SDZ and a series of mono- and bipyridines. The solids are achieved using our co-crystal screening technique based on solution-mediated phase transformation (SMPT).[16] The pyridines comprise *N*,*N*-dimethyl-4-aminopyridine (dmap), 4-aminopyridine (4-ap), 4-picoline (pico), 4,4′-bipyridine (bipy), *trans*-1,2-bis(4-pyridyl)ethylene (bpe), 1,2-bis(4-pyridyl) acetylene (bpa), and 4-(pyridin-4-yl)piperazine (4-pypip) (Scheme 2). The resultant solids involve both co-crystals and salts that, we show, provide innovative insights into the co-crystal−salt continuum.[17] The co-crystals and salts are sustained by three primary hydrogen-bond motifs involving heterodimers, rings, and/or chains based

Scheme 2. Pyridine Co-Formers Employed in Solid-State Complexes Involving SDZ

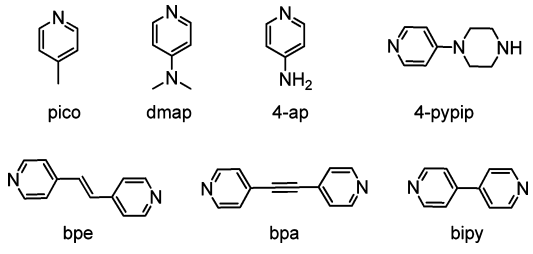

upon five of Etter's graph sets.[18] The co-formers that preserve the amidine−pyrimidine dimer, namely, bpe and bpa, also afford novel "host−guest" solids, wherein the pyridine only interrupts the formation of secondary N−H···O_2S synthons.

From our efforts to investigate the co-crystal−salt continuum of complexes involving SDs,[17] we demonstrate two salient observations. First, each solid can be classified as a co-crystal or salt according to the geometry of the sulfonamide. More specifically, an analysis of our solids along with reported SD complexes reveals trends between S−N bond length and nature of complex formed, with longer and shorter S−N bond lengths being present in neutral and anionic (i.e., salts) SDs, respectively. Whereas effects of proton transfer on C−O bond length have, for example, been well-established in RCO_2H/RCO_2^- systems,[19] an analysis of S−N bond geometry as related to co-crystals and salts has not been reported. Second, we reveal how tautomers of SDs can play a heretofore unaddressed role in supporting the formation of co-crystals as related to the co-crystal−salt continuum.[17] Tautomers are constitutional isomers that rapidly interconvert by a chemical reaction between two or more forms.[20] A tautomeric form of a molecule can, in principle, be either neutral or charged (i.e., cation or anion), while recent reviews suggest that the majority of tautomers present in the solid state exist as a neutral form.[21] Here, we demonstrate that while those tautomers of SDs isolated in the solid state to date fall within the co-crystal regime, the geometries of the higher-energy imidine tautomers lie *effectively at the co-crystal−salt boundary*.[17] From a crystal engineering perspective, such an observation is consistent with a SD being able to assume more "salt-like" behavior in order to achieve a crystal lattice. Moreover, given that different tautomers of a molecule can also be expected to form different supramolecular synthons in solids,[20] tautomers can be considered to exhibit chameleon-like behavior in the solid state by assuming forms that both promote crystal formation and conform to geometric demands of different co-former components. We expect the identification of such a role of tautomers in supporting the formation of co-crystals to extend our general understanding of the nature of the co-crystal−salt continuum.

Materials. SDZ (98%) and pico (98%) were purchased from Alfa Aesar and used without further purification. dmap (98%), 4-ap (98%), bipy (97%), and bpe (98%) were purchased from Aldrich Chemical Co. and used after recrystallization. 4-pypip (97%) was purchased from Matrix Scientific and used without further purification. bpa was synthesized according to a literature procedure.[22]

Single Crystal Preparation. Single crystals of each solid were obtained by slow evaporation from solution. In a typical procedure, SDZ (4 mmol) and pyridine (1.0 mol equiv for monopyridines, and 0.5 mol equiv for bipyridines) were dissolved in DMF at 85 °C. Single crystals suitable for X-ray diffraction were grown upon cooling each solution to ambient temperature and then allowing the solvent to slowly evaporate. Single crystals formed within a period of approximately 10 days.

Single Crystal X-ray Crystallography. Single crystal X-ray diffraction experiments were performed on a Bruker SMART system equipped with an APEX2 CCD camera (co-formers: pico, bipy, bpe, bpa, 4-pypip), or on a Nonius Kappa CCD diffractometer (co-formers: dmap and 4-ap). Data was collected at 100 or 293 K with graphite-monochromated MoK_α radiation (λ = 0.71073 Å). The data were collected and processed using either SaintPlus[23] (co-formers: pico, bipy, bpe,

dx.doi.org/10.1021/cg301745x | *Cryst. Growth Des.* 2013, 13, 393−403

bpa, 4-pypip), or a combination of Collect[24] and HKL Scalepack/Denzo[25] (co-formers: dmap and 4-ap). All structures were solved using direct methods that generated non-hydrogen atoms. All hydrogen atoms were located in Fourier-difference electron density maps. All non-hydrogen atoms were refined anisotropically. Hydrogen atoms associated with carbon atoms were refined in geometrically constrained riding positions. Hydrogen atoms associated with nitrogen atoms were included in the located positions. Refinement was achieved with the use of SHELX-97.[26]

Cambridge Crystallographic Database Search. The CSD database survey was accomplished using version 5.32 (including update 5, November 2011) with ConQuest[37] (version 1.13). The CSD was searched for mono-N-substituted sulfonamides comprising a sulfanilamide substructure that satisfies the following criteria: (a) crystallographic R factor < 0.075, (b) not polymer structure,[28] (c) not powder structure, (d) 3D coordinates fully determined, and (e) purely organic components.[29]

Statistical Analysis of Salts and Co-Crystals. The regions of those parameters (i.e., S−N length, SNC angle) that support salt or co-crystal formation were analyzed by calculating the mean ($\bar{X}$) and standard deviation (σ) for each variable. The calculated σ values for S−N length of each complex type were generally low in comparison to the range of observed values (S−N range =0.089 Å; σ_{salt} = 0.007 Å (7.9%); $\sigma_{co\text{-}crystal}$ = 0.018 Å (20.2%)), the σ values for SNC angle were much larger (SNC range =9.53°; σ_{salt} = 2.55° (26.8%); $\sigma_{co\text{-}crystal}$ = 1.83° (19.2%)). The SNC angles displayed more variation; thus, S−N lengths were used to assess salt and co-crystal regions. The boundaries for each region are depicted such that each region represented $\bar{X} \pm 2\sigma$.

RESULTS

Seven solid forms of SDZ were realized through screening[16] with pyridines. The crystal structure of each solid was determined using single-crystal X-ray diffraction. Four solids were determined to be co-crystals, while the remaining three solids were salts, evidenced by proton transfer. In each SDZ solid, the sulfonamide crystallizes as either an amidine or amidide for co-crystals and salts, respectively.

(1). (SDZ)·(pico). (SDZ)·(pico) crystallizes from neat pico in the triclinic space group $P\bar{1}$. The asymmetric unit consists of one molecule of SDZ and one molecule of pico (Figure 1a). The components interact in a discrete assembly *via* (amidine) N−H···N (pyridine) hydrogen bonds that constitute a $D_1^1(2)$ graph set. The assembly is sustained by intermolecular (aniline) N−H···N (pyrimidine) interactions between face-to-face stacked SDZ molecules in a $R_2^2(20)$ ring. The N−H group also participates in a weak hydrogen bond with the SO_2 group ($d_{N\cdots O}$ = 3.34 Å), which lies slightly beyond cited cutoff values for significant hydrogen bonding.[8] Additional $\pi\cdots\pi$ interactions between adjacent aniline rings ($d_{\pi\cdots\pi}$ = 3.23 Å) contribute to the extended packing (Figure 1b).

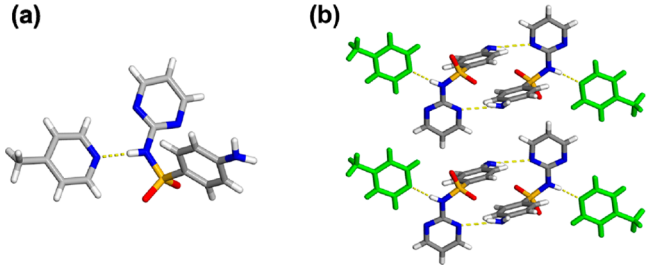

Figure 1. View of (SDZ)·(pico): (a) primary synthon and (b) extended structure highlighting (aniline) N−H···N (pyrimidine) hydrogen bonds and $\pi\cdots\pi$ interactions between adjacent aniline rings.

(2). 2(SDZ)·3(bipy). Co-crystallization of a 2:1 molar ratio of SDZ and bipy from DMF produces a co-crystal of 2:3 stoichiometry, respectively. The components crystallize in the triclinic space group $P\bar{1}$ with two molecules of SDZ and three molecules of bipy in the asymmetric unit. SDZ and bipy interact *via* intermolecular (amidine) N−H···N (pyridine) and (aniline) N−H···N (pyridine) hydrogen bonds. The components form a 2D polymer sustained by a chain of sulfonamide and aniline N−H···N hydrogen bonds, as well as (aniline) N−H···O_2S (sulfoxide) forces based on a C(8) graph set (Figure 2). The N−H···O_2S interactions link each SDZ in the heteromolecular chain to individual (bipy)-(SDZ)-(bipy) "bridges" that join two parallel chains, wherein each bipy participates in a single hydrogen bond with a "free" pyridine in each unit. The free pyridines interact with the main chain aniline groups *via* C−H···N forces ($d_{C\cdots N}$ = 3.38 Å). In each molecule of bipy, the pyridines are twisted ca. 31−33° from coplanarity and participate in face-to-face $\pi\cdots\pi$ interactions ($d_{\pi\cdots\pi}$ = 3.35, 3.38, and 3.69 Å) with the stacked bipy molecules.

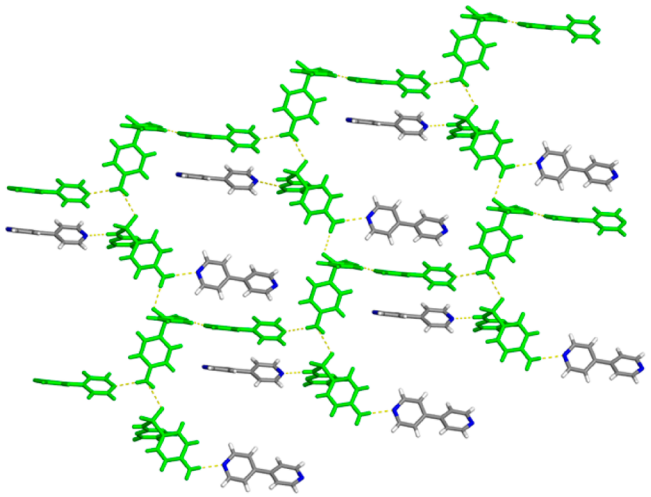

Figure 2. View of 2(SDZ)·3(bipy) showing polymer backbone (green) and hydrogen bonds.

(3). 2(SDZ)·(bpe). 2(SDZ)·(bpe) crystallizes from DMF in the triclinic space group $P\bar{1}$ with one molecule of SDZ and a 1/2 bpe molecule in the asymmetric unit. SDZ and bpe form a 2D hydrogen-bonded polymer. The components interact *via* intermolecular (aniline) N−H···N (pyridine) hydrogen bonds, which constitute a $D_1^1(2)$ graph set (Figure 3). The

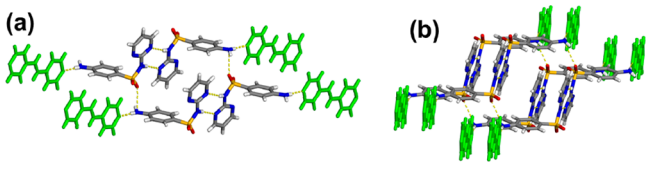

Figure 3. View of 2(SDZ)·(bpe) highlighting: (a) amidine−pyrimidine dimers and (b) $\pi\cdots\pi$ interactions between adjacent pyrimidine rings and pyridine co-formers.

dx.doi.org/10.1021/cg301745x | Cryst. Growth Des. 2013, 13, 393−403

sulfonamide -NH group participates in dimer formation with a second molecule of SDZ that is based on a $R_2^2(8)$ array of (amidine) N−H···N (pyrimidine) interactions. The NH_2 group of SDZ is involved in an intermolecular N−H···O_2S hydrogen bond. Additional $\pi\cdots\pi$ interactions between adjacent pyrimidine rings ($d_{\pi\cdots\pi}$ = 3.63 Å) and stacked pyridines ($d_{\pi\cdots\pi}$ = 3.43 Å) contribute to the extended structure.

(4). 2(SDZ)·(bpa). SDZ and bpa co-crystallize from DMF in the triclinic space group $P\bar{1}$ with one molecule of SDZ and a 1/2 bpa molecule in the asymmetric unit. The components form a 2D hydrogen-bonded polymer held together by (aniline) N−H···N (pyridine) hydrogen bonds. SDZ and bpa assemble similar to 2(SDZ)·(bpe) wherein adjacent SDZ molecules form hydrogen-bonded dimers *via* (amidine) N−H···N (pyrimidine) forces in a $R_2^2(8)$ ring. The NH_2 group of SDZ also participates in intermolecular N−H···O_2S hydrogen bonds (Figure 4). Additional $\pi\cdots\pi$ interactions are present between stacked pyrimidine ($d_{\pi\cdots\pi}$ = 3.66 Å) and pyridine rings ($d_{\pi\cdots\pi}$ = 3.50 Å).

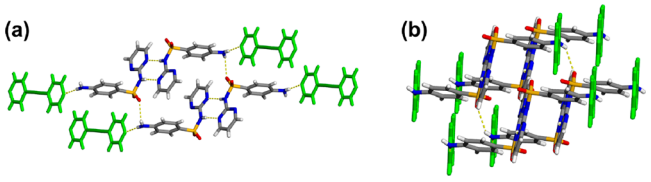

Figure 4. View of 2(SDZ)·(bpa) highlighting: (a) amidine-pyrimidine dimers and (b) $\pi\cdots\pi$ interactions between adjacent pyrimidine rings and pyridine co-formers.

(5). (dmap$^+$)·(SDZ$^-$). SDZ and dmap form a salt that crystallizes in the monoclinic space group $P2_1/n$ with one dmap$^+$ cation and one SDZ$^-$ anion in the asymmetric unit. The components form a 2D hydrogen-bonded assembly linked *via* a primary intermolecular (pyridinium) $^+$N−H···N$^-$ (amidide) hydrogen bond (Figure 5a). The extended structure is sustained by intermolecular N−H···O_2S interactions, as well as face-to-face $\pi\cdots\pi$ interactions between pyrimidine rings ($d_{\pi\cdots\pi}$ = 3.29 Å) (Figure 5b).

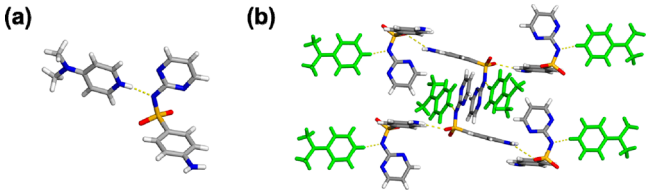

Figure 5. Views of (dmap$^+$)·(SDZ$^-$): (a) primary interaction and (b) extended structure.

(6). (4-ap+)·(SDZ$^-$). SDZ and 4-ap form a salt that crystallizes from DMF in the monoclinic space group $P2_1/c$. The asymmetric unit consists of one 4-ap$^+$ cation and one SDZ$^-$ anion that assemble *via* intermolecular (pyridinium) $^+$N−H···N$^-$ (amidide) and (aminopyridine) N−H···O_2S (sulfoxide) hydrogen bonds in a $R_2^2(20)$ ring (Figure 6a). The components form a 2D polymer with $\pi\cdots\pi$ interactions between pairs of stacked pyrimidine and pyridine rings ($d_{\pi\cdots\pi}$ = 3.80 Å) (Figure 6b).

(7). (4-pypip$^+$)·(SDZ$^-$). SDZ and 4-pypip form a salt that crystallizes from DMF in the monoclinic space group $P2_1/n$. The asymmetric unit consists of one 4-pypip$^+$ cation and one SDZ$^-$ anion that self-assemble to form a 3D hydrogen-bonded

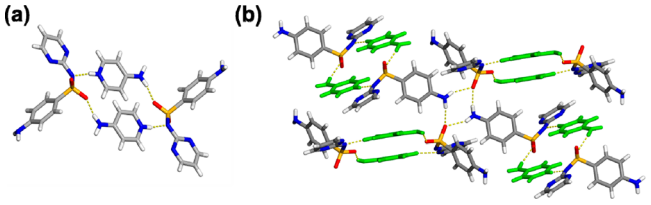

Figure 6. Views of (4-ap$^+$)·(SDZ$^-$): (a) primary interaction and (b) extended structure.

polymer. Intermolecular (pyridinium) $^+$N−H···N$^-$ (amidide) and (amine) N−H···O_2S (sulfoxide) hydrogen bonds in a $C_2^2(13)$ chain, as well as (aniline) N−H···O_2S (sulfoxide) forces in a C(8) chain, form a 2D network (Figure 7). The NH_2 of SDZ$^-$ is also involved in an array of (aniline) N−H···N (pyrimidine) hydrogen bonds in a $R_2^2(20)$ graph set.

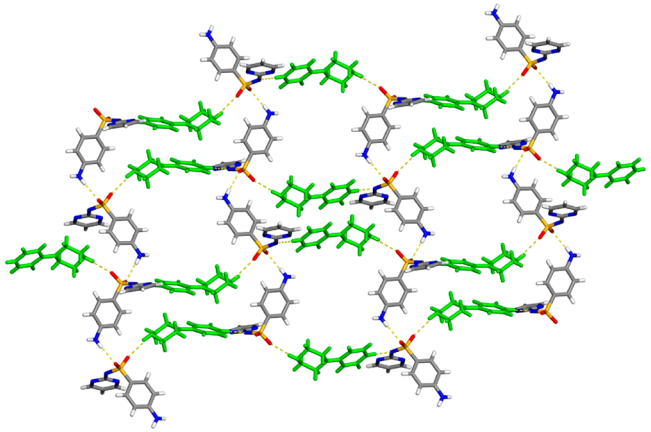

Figure 7. View of (4-pypip$^+$)·(SDZ$^-$): 2D network of $^+$N−H···N$^-$ and N−H···O_2S hydrogen bonds.

DISCUSSION

Co-crystallization strategies to disrupt dimer formation and generate multicomponent solids have been reported with CBZ.[5] The goal was realized using carboxylic acids that act as stronger hydrogen-bond-donors and compete with CBZ dimer formation through (acid) O−H···O═C (amide) hydrogen bonds.[30] The work involving CBZ suggested to us that a similar

Scheme 3. Approaches to Multicomponent Solids Involving SDZ and Pyridines: (a) Monopyridyl Co-Formers, (b) Bipyridyl Co-Formers, and (c) Pyridine Co-Formers with Hydrogen-Bond-Donor (HD) Groups

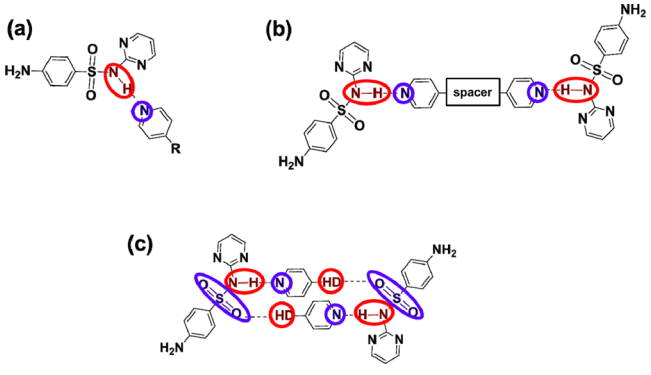

dx.doi.org/10.1021/cg301745x | Cryst. Growth Des. 2013, 13, 393−403

Scheme 4. pK_a Values of Co-Formers in Relation to SDZ[a]

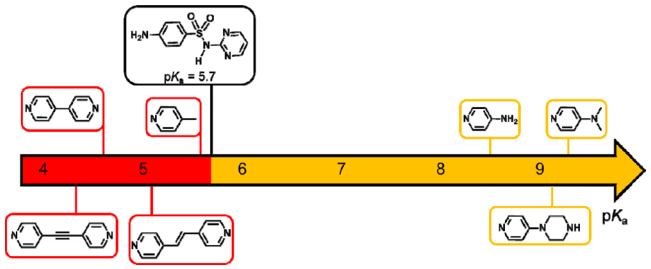

[a]Red region depicts co-formers that facilitated co-crystal formation and yellow facilitated proton transfer.

Scheme 5. Finite Graph Sets with Pyridine Co-Formers (Occurrences in Blue)

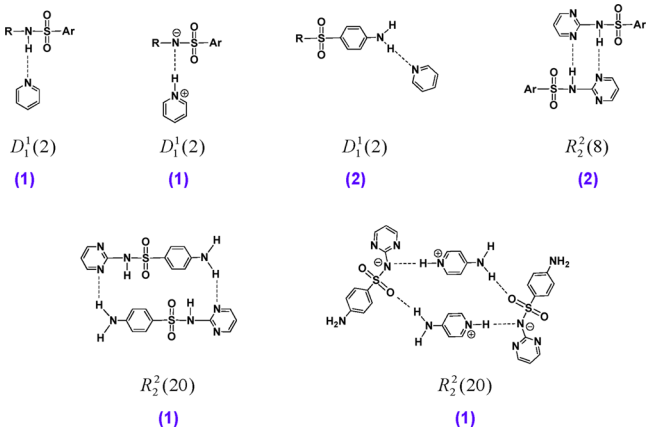

Scheme 6. Chains with Pyridine Co-Formers (Occurrences in Blue)

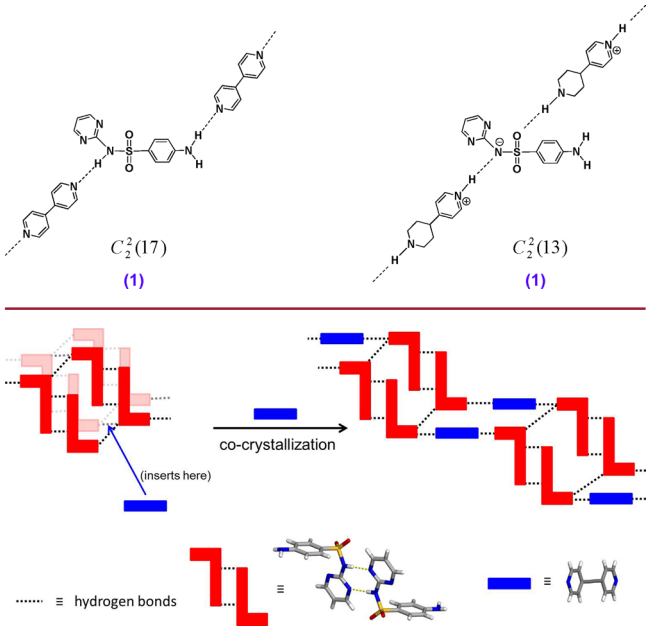

Figure 8. Schematic of interactions in pure SDZ and the "host–guest" co-crystal with bpa.

strategy could be applied in the case of SDZ and pyridines (Scheme 3a,b). Specifically, pyridine co-formers would provide a sufficient hydrogen-bond-acceptor to interact with the

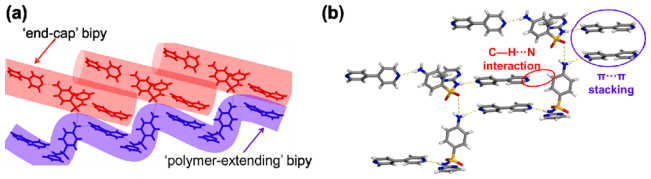

Figure 9. Co-crystal 3(SDZ)·2(bipy) highlighting: (a) "end-cap" and (b) "polymer-extending" bipys and secondary interactions with unbound ends of bipy molecules.

Scheme 7. Schematic of Sulfonamide Geometries in (a) Anionic and (b) Neutral Forms

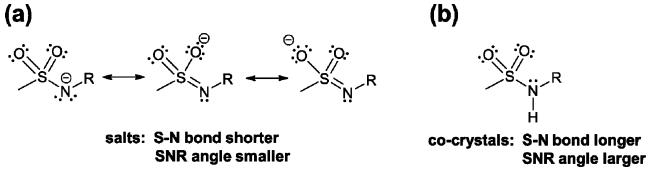

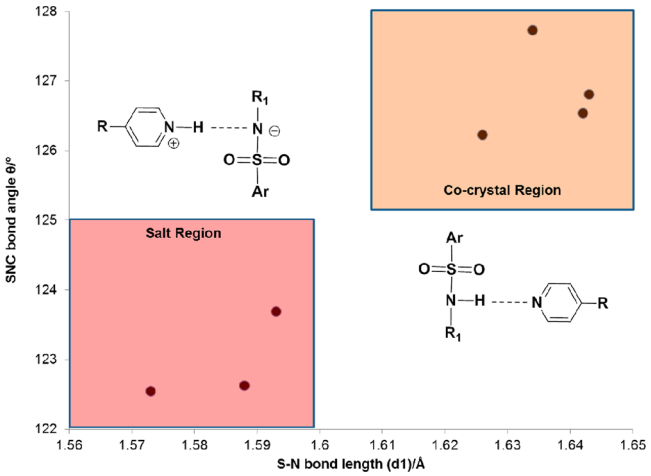

Figure 10. S–N bond length vs SNC angle for SDZ-based solids.

sulfonamide N–H while breaking the dimer. The relative acidity of SDZ (pK_a = 5.69)[31] can facilitate proton transfer to a pyridine N-atom to disrupt dimer formation.

In this context, an investigation of the CSD revealed 35 co-crystals and 8 salts that comprise a SD.[32] The majority of structures contain either an (amidine) N–H···O=C (carbonyl) (16 hits) or a (pyrimidinium) $^+$N–H···N$^-$ (amidide) (8 hits) hydrogen bond as a primary interaction between the components. Most complexes contain secondary interactions in the form of N–H···O_2S hydrogen bonds between two SD molecules, which suggested that the sulfoxide group can be integrated into hydrogen-bonded motifs of supramolecular complexes of pyridines (Scheme 3c). The sulfoxide has very recently emerged as a group able to sustain synthon formation in solids.[7c]

More specifically, SDZ possesses hydrogen-bond-donor and -acceptor groups that make the molecule an attractive target for crystal engineering. The -NH_2 and -NH groups are donors, while the pyrimidine N-atoms and -SO_2 group are acceptors. The relative proximity of the sulfonamide -NH group to both the acceptor sulfoxide and pyrimidine ring also makes the molecule exploitable for two-point synthons.[14] As stated, two-point synthons based on (amidine) N–H···N (pyrimidine) forces sustain the hydrogen-bonded dimer of SDZ. Similar two-

dx.doi.org/10.1021/cg301745x | Cryst. Growth Des. 2013, 13, 393–403

Table 1. Geometric Parameters for Our and Previously Reported SD-Based Complexes

entry	sulfa drug	co-former	θ/°	d1/Å	co-crystal/salt	reference
1	sulfamethoxypyridazine	trimethoprim, H_2O	125.19	1.571	salt	41
2	sulfadiazine	ampyr	122.55	1.573	salt	this work
3	sulfamethoxazole	trimethoprim	123.47	1.573	salt	42
4	sulfametrole	tetroxoprim, MeOH	118.83	1.576	salt	43
5	sulfametrole	tetroxoprim, H_2O	119.43	1.577	salt	43
6	sulfametrole	tetroxoprim, H_2O	119.63	1.581	salt	43
7	sulfamethazine	4-hydroxybenzamide	122.80	1.584	co-crystal[a]	10b
8	sulfametrole	tetroxoprim, EtOH	118.20	1.585	salt	43
9	sulfametrole	trimethoprim	118.30	1.585	salt	44
10	sulfamethazine	4-hydroxybenzamide	123.26	1.585	co-crystal[a]	10b
11	sulfadiazine	4-pypip	122.63	1.588	salt	this work
12	sulfadiazine	dmap	123.69	1.593	salt	this work
13	sulfamethoxypyridazine	trimethoprim	121.68	1.598	co-crystal[a]	41
14	sulfamethazine	picolinamide	121.38	1.602	co-crystal[a]	10b
15	sulfamethazine	4-hydroxybenzoic acid	122.81	1.608	co-crystal[a]	10b
16	sulfamethazine	theopylline	120.13	1.618	co-crystal[a,b]	45
17	sulfamethazine	trimethoprim, MeOH	124.22	1.622	co-crystal	46
18	sulfamethazine	indole-2-carboxylic acid	125.55	1.623	co-crystal	47
19	sulfamethazine	4-aminosalicylic acid	125.32	1.624	co-crystal	48
20	sulfadiazine	4-pico	126.23	1.626	co-crystal	this work
21	sulfamethazine	4-aminobenzoic acid	123.58	1.627	co-crystal	49
22	sulfamethazine	2,4-dihydroxybenzoic acid	126.98	1.628	co-crystal	47
23	sulfamethazine	3-hydroxy-2-naphthoic acid	121.40	1.629	co-crystal[a]	10b
24	sulfadiazine	bipy	127.73	1.634	co-crystal	this work
25	sulfamethazine	fumaric acid, CH_3CN	125.84	1.635	co-crystal	10b
26	sulfamethazine	4-chlorobenzoic acid	124.74	1.637	co-crystal	50
27	5-methoxysulfadiazine	acetylsalicylic acid	124.05	1.641	co-crystal	51
28	sulfamethazine	salicylic acid	126.58	1.641	co-crystal	52
29	sulfamethazine	2-aminobenzoic acid	125.92	1.641	co-crystal	49
30	sulfamethazine	theophylline	125.78	1.642	co-crystal[b]	45
31	5-methoxysulfadiazine	(18-C-6), CH_3CN	125.88	1.642	co-crystal	53
32	sulfadiazine	bpe	126.54	1.642	co-crystal	this work
33	sulfamethazine	acetylsalicylic acid	125.94	1.643	co-crystal	48
34	sulfadiazine	bpa	126.81	1.643	co-crystal	this work
35	sulfapyridine	oxalic acid, dibutyl ester	122.79	1.644	co-crystal	54
36	sulfamethazine	3,4-dichlorobenzoic acid	126.92	1.644	co-crystal	10b
37	sulfamethazine	sorbic acid	127.15	1.644	co-crystal	10b
38	sulfamerazine	(18-C-6), CH_3CN	125.65	1.645	co-crystal	53
39	5-methoxysulfadiazine	dioxane	126.23	1.646	co-crystal	55
40	sulfamethazine	MeOH	124.78	1.647	co-crystal	56
41	sulfamethazine	trimethoprim, H_2O	125.49	1.647	co-crystal	57
42	chlorsulfaquinoxaline	CH_3CN	124.62	1.648	co-crystal	58
43	5-methoxysulfadiazine	THF	125.55	1.648	co-crystal	55
44	sulfamethazine	2,4-dinitrobenzoic acid	126.18	1.650	co-crystal	47
45	sulfamethazine	salicylic acid	126.20	1.651	co-crystal	59
46	*N*-acetylsufanilamide	caffeine	124.85	1.652	co-crystal	60
47	sulfamethazine	benzoic acid	126.54	1.652	co-crystal	61
48	sulfamethazine	saccharin	125.56	1.656	salt[c]	62
49	sulfamethazine	1-hydroxy-2-naphthoic acid	126.77	1.658	co-crystal	10b
50	sulfaproxyline	caffeine	124.39	1.660	co-crystal	63

[a]Denotes complexes containing the imidine tautomer of the sulfonamide. [b]Entries found in same crystal structure. [c]Denotes salt containing a cationic SD and anionic co-former (excluded from geometry study).

point interactions involving pyrimidines are prevalent in the field of molecular recognition and play a prominent role in biology.[33] The introduction of pyridine co-formers that compete with dimer formation can also facilitate the formation of additional intermolecular forces (e.g., (amidine) N−H···O_2S (sulfoxide)). SDZ, thus, represented an attractive model SD for studies of synthon hierarchies and to generate supramolecular complexes sustained by different hydrogen-bond patterns.

Co-Crystals and Salts. Given that the pK_a of pyridine is larger than pyrimidine (pK_a = −1.3),[31] we expected the pyridine co-formers to interact with the sulfonamide either *via* neutral N−H···N interactions or involve proton transfer. Four of the seven co-formers afforded co-crystals while three

dx.doi.org/10.1021/cg301745x | *Cryst. Growth Des.* 2013, 13, 393−403

Scheme 8. Schematic of Tautomers of SMT

generated salts (Scheme 4). A division of co-crystals and salts can be assigned using the ΔpK_a of the components.[17] For the co-formers, $\Delta pK_a < 0$ resulted in co-crystal formation, while $\Delta pK_a > 0$ resulted in proton transfer. Indeed, being able to recognize combinations of components that exhibit both salt and co-crystal formation is important when assembling specific supramolecular architectures, as recently discussed by Aakeröy.[34]

Motifs and Graph Sets. There are a wide variety of commercially available and synthetically accessible pyridines (pK_a pyridine = 5.2)[35] that can be used to disrupt dimer formation of SDZ while supporting the formation of a either a co-crystal or salt.[17] Complexes formed using a wide range of pyridines would not only provide a means to investigate how pK_a influences co-crystal or salt formation in SD-based solids but also support different supramolecular synthons in resulting complexes.

While SDZ contains more hydrogen-bond-acceptor than -donor groups, the use of pyridine co-formers adds to an imbalance of acceptors and, thus, could be expected to expand the number and kinds of motifs in the resulting solid-state complexes.[9a] In five out of seven solids, the pyridine co-former interrupted dimer formation. For the co-crystals, the dimer of SDZ was both disrupted and maintained. Whereas both pico and bipy disrupted the dimer, solids involving bpe and bpa maintained the (amidine) N−H···N (pyrimidine) synthon. For the more basic pyridines (i.e., 4-ap, dmap, 4-pypip), dimer disruption was accompanied by proton transfer to the pyridine N-atom.

Five different graph sets are ascribed to the solids isolated in this study, namely, $D_1^1(2)$ dyad, $R_2^2(8)$ ring, $R_2^2(20)$ ring, $C_2^2(17)$ chain, and $C_2^2(13)$ chain (Scheme 5), with the dyads and rings representative of discrete motifs. The most frequent pattern is a single interaction between either the amido or amino N−H of SDZ and the pyridine N-atom, described by the $D_1^1(2)$ notation. The pattern occurred in four out of seven solids, with one of three synthons. Specifically, (amidine) N−H···N (pyridine), (aniline) N−H···N (pyridine), and (pyridinium) $^+$N−H···N$^-$ (amidide) hydrogen bonds comprise the $D_1^1(2)$ graph set. The $R_2^2(8)$ ring describes the two-point interaction present between the sulfonamide and pyrimidine ring that affords the dimer. The two structures that contain the hydrogen-bonding ring also result in interactions between the aniline N−H and pyridine N-atom, being classified as $D_1^1(2)$ notation. The $R_2^2(20)$ ring is present in two different types, each being promoted by a "bidentate" nature of SDs. Specifically, a homomolecular ring[36] sustained by (amidine) N−H···N (pyridine) hydrogen bonds is present in (SDZ)·(pico), while a heteromolecular ring is present in (4-ap$^+$)·(SDZ). The hydrogen-bond pattern in the salt (4-ap$^+$)·(SDZ$^-$) is based on an array of (pyridinium) $^+$N−H···N$^-$ (amidide) and (amine) N−H···O_2S (sulfoxide) forces.

The remaining motif is a heteromolecular chain in 2(SDZ)·3(bipy) (Scheme 6). In the solid, SDZ interacts with bipy at both hydrogen-bond-donor sites to give a $C_2^2(17)$ chain. Notably, the salt (4-pypip$^+$)·(SDZ$^-$) demonstrates similar structural behavior to 2(SDZ)·3(bipy) despite the addition of a donor site in the form of the piperazine group. Salt formation results in the 4-pypip$^+$ cation interacting with the strongest two acceptor sites of SDZ, affording a $C_2^2(13)$ chain. Both structures also contain homomolecular C(8) chains between aniline N−H and SO_2 groups.[9a]

"Host−Guest" Co-Crystals. In both 2(SDZ)·(bpe) and 2(SDZ)·(bpa), the co-former competed with secondary hydrogen-bond synthons so as to enable the amidine−pyrimidine $R_2^2(8)$ ring dimer to be preserved. Both bipyridines, however, disrupted the formation of N−H···O_2S hydrogen bonds that link pairs of dimers in pure SDZ (Figure 8). Thus, effectively half of the N−H···O_2S interactions were retained in both solids. Both co-crystals also contain face-to-face π···π

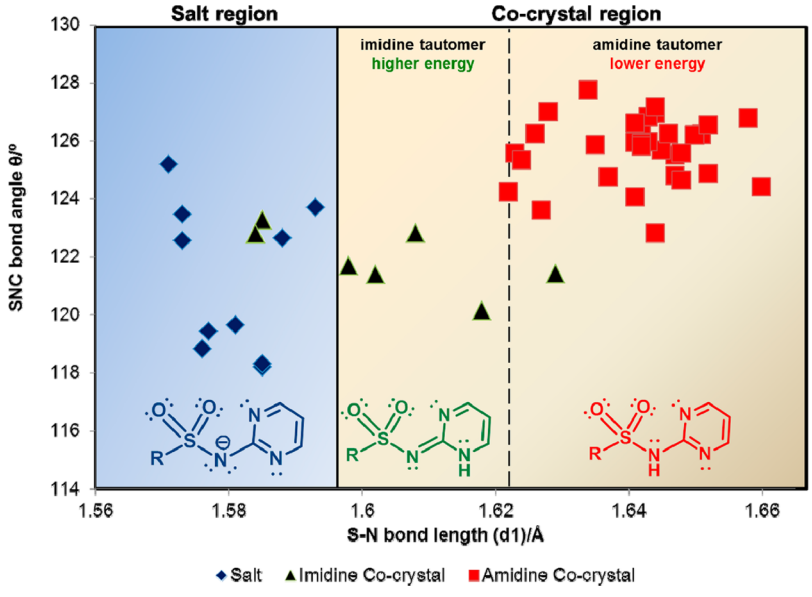

Figure 11. A plot of S−N bond length vs SNC bond angle for SD-based complexes.

dx.doi.org/10.1021/cg301745x | Cryst. Growth Des. 2013, 13, 393−403

interactions between adjacent stacks of dimers that are analogous to those in pure SDZ, as well as additional $\pi\cdots\pi$ interactions between stacked pyridines. Consequently, the co-formers are akin to guest molecules within host lattices wherein the bipyridines are inserted into frameworks that do not disturb primary interactions in pure SDZ. Surprisingly, the "better donor" (i.e. amidine N−H) does not form a hydrogen bond with the "better acceptor" (i.e., pyridine N-atom) in each solid.[37] Energy differences between the two different hydrogen-bond motifs (e.g., ring dimer and expected chain) may be minimal and overcome by more favorable close packing forces.

Unexpected Stoichiometry. The co-crystal involving SDZ and bipy is unexpected in terms of stoichiometry. Specifically, an as-prepared 2:1 ratio of SDZ and bipy co-crystallized as 2(SDZ)·3(bipy) to give a mixed assembly with both the amidine N−H group and aniline N−H group participating in hydrogen bonds. Within the co-crystal, there are two distinct "classes" of bipy molecules. The first type of bipy participates in two different N−H···N interactions that extend the polymer framework (Figure 9a, polymer-extending bipy). The second type comprises the pendant (bipy)-(SDZ)-(bipy) units and form hydrogen bonds to the strong donor. The pendant bipy molecules each contain a pyridyl group that does not participate in a hydrogen bond. The pyridine unit that serves to effectively end-cap a polymer chain (Figure 9a, end-cap bipy). The free pyridyl group, instead, participates in C−H···N forces with an adjacent SDZ molecule (Figure 9b).

A search of the CSD reveals that free 4-pyridyl groups of bipy molecules and corresponding co-formers similar to SDZ (i.e., contains strong hydrogen-bond donors, such as OH or NH) have been reported.[38] A total of 248 solids are observed with only 16 (6.45%) that possess a bipy molecule with only one 4-pyridyl group participating in a hydrogen bond.[39] Similar to 2(SDZ)·3(bipy), the bipy molecules will often participate in weak C−H···N or C−H···π forces.[38]

Geometry of the Sulfonamide: A CSD Study. Although SDs are gaining interest as building blocks in crystal engineering,[10] less effort has been extended to compare SD-based co-crystals and salts involving a series of co-formers. Having generated both co-crystals and salts of SDZ, we examined the solids with a view to understand geometric changes associated with the sulfonamide moiety. Proton transfer from a SD was expected to result in an increase of the sp^2 character of the sulfonamide N-atom and, thus, lead to a decrease in the S−N bond length and, concomitantly, smaller SNR bond angle (i.e. higher S═N character) (Scheme 7). Conversely, co-crystals were expected to exhibit longer S−N bond lengths and larger SNR bond angles. The geometry of biologically active sulfonamides has been examined in the gas phase and compared to the anionic form.[40] Computational studies reveal the sulfonamide group to exhibit partial S═N character upon deprotonation.

From our work involving pyridines, the S−N bond lengths and S−N−C (pyrimidine) angles were different for salts and co-crystals. The salts exhibited shorter S−N bond lengths with a range of 1.56−1.60 Å, which is consistent with greater S═N character. The co-crystals exhibited longer S−N bonds with a range of 1.61−1.65 Å. Additionally, the SNC bond angles were appreciably smaller for salts (122−124°) as compared to co-crystals (126−128°). Collectively, the geometry of the sulfonamide moiety enables the co-crystals and salts reported here to be delineated (Figure 10). We, thus, conclude that both S−N bond length and SNC angle can guide the identification of multicomponent solids based on SDZ as being either a co-crystal or salt.

We next turned to the CSD to examine related SD-based solids. A search of the CSD revealed 42 multicomponent solids involving 10 SDs, with 34 (81%) being co-crystals and 8 (19%) being salts. The majority of co-formers were based on *N*-heterocyclic amines (10) and carboxylic acids (18), as well as amides (4) and xanthines (3). One pyridine, namely, picolinamide, was employed to generate a co-crystal in the form of (sulfamethazine)·(picolinamide). The components are sustained by (amidine) N−H···O═C (carbonyl) forces and the pyridine participates in secondary (alkyl) C−H···N (pyridine) forces. In 24 complexes, the co-former interacts with the sulfonamide N−H group *via* either (amidine) N−H···N (pyrimidine) or (amidine) N−H···O═C (carbonyl) forces in a two-point interaction.

The S−N bond lengths and SNC angles of our pyridine-based co-crystals and salts generally fall within the ranges of the reported SD complexes (Table 1). The S−N bond lengths and sulfonamide SNC angles of the reported complexes range from 1.56 to 1.67 Å and 118 to 127°, respectively. The larger differences compared to our SDZ-based solids can be attributed to the larger variety of co-formers and sample size, since different SDs and co-formers can be expected to accommodate a wider array of S−N lengths and SNC angles. Indeed, the SDs differ in electronic character of the R group (R = pyridazine, pyrimidine, oxazole, thiadiazole, quinoxaline, and acetyl). The different R groups are expected to affect delocalization involving the sulfonamide N-atom, and in turn, affect S═N character.

The SD-based solids in the CSD reveal that the salts exhibit S−N bond lengths of 1.57−1.60 Å, while co-crystals exhibit S−N bond lengths of 1.58−1.66 Å. In contrast to our pyridine-based solids, there is slight overlap in S−N bond distances of the reported salts and co-crystals from 1.58 to 1.60 Å. The overlap involves five co-crystals and six salts. The SNC angles ranged from 118 to 125° for salts and 120 to 128° for co-crystals. There is, thus, also overlap of SNC bond angles from 120 to 125°. The solids in that region comprise 17 co-crystals and four salts. As discussed by Childs in the context of C−O bond length and ΔpK_a,[17] such an overlap is likely representative of a boundary between co-crystal and salt formation.

Tautomers in the Co-Crystal−Salt Continuum. From our analysis of the 34 SD-based co-crystals in the CSD, seven sulfonamides (~21%), in contrast to our co-crystals, exist as the imidine tautomer. The tautomer is present in six of the sulfamethazine (SMT) co-crystals and one co-crystal of sulfamethoxypyridazine. Both SDs contain an *N*-heterocyclic ring atom adjacent to the sulfonamide and can generate two tautomers (Scheme 8). Relative energies of tautomeric forms have been investigated in the case of SMT. DFT calculations reveal the amidine form to be more stable than the imidine form by 33.2 kJ mol^{-1}.[45] The higher energy of the imidine form has been attributed to less aromatic character of the adjacent pyrimidine ring.[45] It has also been suggested that secondary interactions between a co-former and a given sulfonamide will likely influence whether the imidine amidine tautomer forms in a co-crystalline solid.[10b,45]

From a geometric standpoint, the seven co-crystals involving the higher-energy imidine tautomer possess S−N bond lengths and SNC angles of 1.58−1.63 Å and 120−124°, respectively. The remaining 28 co-crystals in the CSD, along with our co-crystals, which are all based upon the amidine tautomer, exhibit

S−N bond lengths of 1.62−1.66 Å. The SNC bond angles of the amidine co-crystals range from 122 to 128°. In comparison, our salts and salts present in the CSD exhibit S−N lengths of 1.57−1.60 Å and SNC angles of 118−125°.

It is clear from the X-ray data that the ranges of S−N length for salts and amidine co-crystals do not overlap (Figure 11). Remarkably, however, effectively *all of the S−N lengths of the imidine − or higher energy tautomer − sit in between the S−N lengths of salts and the amidine tautomer.* The observation is supported by an analysis of S−N bond lengths of the different types of complexes. Using the mean ($\bar{X}$) S−N length and standard deviation (σ) for co-crystals and salts, we analyzed the S−N distribution regions represented by $\bar{X} \pm 2\sigma$. From the data, the salt region covered a range of 1.571−1.593 Å, while the co-crystal region covered 1.594−1.673 Å. The range for S−N bond length of amidine co-crystals was 1.622−1.660 Å; thus, the imidine−amidine boundary is assigned at 1.622 Å (Figure 11, dashed line). To our knowledge, such a structural relationship of tautomers as related to the salt−co-crystal boundary has not been reported.

Tautomers: Implications in Solids. The co-crystals of SDs described here (i.e., CSD and our results) reveal that the geometries of the higher-energy imidine tautomers lie between the salts and those amidine co-crystals. The positioning means that the imidine tautomers effectively lie at the co-crystal−salt boundary. We believe that the relative positioning of the imidine tautomers can be considered significant owing to the following. First, different tautomers of the same compound will exhibit different relative energies. The differences in energy will, *de facto*, correspond to forms that exhibit different polarities.[64] From semiempirical calculations involving SMT,[65] for example, we have determined the imidine tautomer to exhibit a larger dipole moment (9.8 D vs 4.9 D) than the amidine tautomer. From a solid-state chemistry perspective, one can envisage that a higher energy (i.e., higher dipole) form of a tautomer may promote the formation of a co-crystal by supporting a more stable crystal lattice[20] or a lattice more akin to that of a salt. Second, molecules that exhibit tautomeric forms may be particularly useful to promote co-crystal formation since the ability to interconvert between forms can accommodate geometric demands of different co-formers. A molecule that exhibits tautomeric forms, thus, can augment the crystallographic landscape[66] by increasing the number of possible synthons able to support a multicomponent solid. Moreover, the ability of tautomers to exhibit such reconfigurable exteriors, or display chameleon-like behavior,[67] may, in effect, be employed to the advantage of the crystal engineer so as to increase the probability of obtaining co-crystals of a given target molecule.

CONCLUSION

We have described seven solid-state complexes (four co-crystals, and three salts) involving SD and pyridine co-formers. The complexes exhibit structural motifs based on (sulfonamide) N−H···N (pyrimidine), (sulfonamide) N−H···N (pyridine), (aniline) N−H···N (pyridine), and (pyridinium) $^{+}$N−H···N^{-} (sulfonamide), and (amine) N−H···O_2S (sulfonamide) hydrogen bonds. We have analyzed existing SD-based complexes for geometric differences upon salt and co-crystal formation and show that salts display shorter S−N bonds owing to the sp^2 nature of the sulfonamide N-atom whereas co-crystals exhibit longer S−N bonds. While the imidine tautomers of SDs are co-crystals, the geometry of the imidine exclusively lies at the co-crystal−salt boundary. Moreover, we anticipate that the identification of a role of tautomers to support multicomponent solids outlined here may provide further insight on understanding and exploiting the co-crystal−salt continuum, particularly as related to co-crystal formation.

ASSOCIATED CONTENT

Supporting Information

Crystallographic information and .cif files of (SDZ)·(pico), 2(SDZ)·(bpe), 2(SDZ)·(bpa), 2(SDZ)·3(bipy), (dmap^{+})·(SDZ^{-}), (4-ap^{+})·(SDZ^{-}), and (4-pypip^{+})·(SDZ^{-}). This material is available free of charge via the Internet at http://pubs.acs.org.

AUTHOR INFORMATION

Corresponding Author

*E-mail: len-macgillivray@uiowa.edu (L.R.M.); geoff.gz.zhang@abbott.com (G.G.Z.Z.).

Notes

The authors declare no competing financial interest.

ACKNOWLEDGMENTS

We are grateful to the National Science Foundation (L.R.M., DMR-1104650) for financial support.

REFERENCES

(1) (a) Desiraju, G. R. *Angew. Chem., Int. Ed.* **1995**, *34*, 2311−2327. (b) Aakeröy, C. B.; Seddon, K. R. *Chem. Soc. Rev.* **1993**, *22*, 397−407. (c) Pace, C. J.; Zheng, H.; Mylvaganam, R.; Kim, D.; Gao, J. *Angew. Chem., Int. Ed.* **2012**, *51*, 103−107. (d) Zuckerman-Schpector, J.; Haiduc, I.; Tiekink, E. R. T. *Chem. Commun.* **2011**, *47*, 12682−12684. (e) Dey, A.; Kirchner, M. T.; Vangala, V. R.; Desiraju, G. R.; Mondal, R.; Howard, J. A. K. *J. Am. Chem. Soc.* **2005**, *127*, 10545−10559. (f) Reddy, R. S.; Craig, D. C.; Desiraju, G. R. *J. Am. Chem. Soc.* **1996**, *118*, 4090−4093.

(2) (a) Kavuru, P.; Aboraryes, D.; Arora, K. K.; Clarke, H. D.; Kennedy, A.; Marshall, L.; Ong, T. T.; Perman, J.; Pujari, T.; Wojtas, L.; Zaworotko, M. J. *Cryst. Growth Des.* **2010**, *10*, 3568−3584. (b) Shattock, T. R.; Arora, K. K.; Vishweshwar, P.; Zaworotko, M. J. *Cryst. Growth Des.* **2008**, *8*, 4533−4545. (c) Bis, J. A.; Vishweshwar, P.; Weyna, D.; Zaworotko, M. J. *Mol. Pharmaceutics* **2007**, *4*, 401−416.

(3) (a) Desiraju, G. R. *Angew. Chem., Int. Ed.* **2007**, *46*, 8342−8356. (b) Bica, K.; Shamshina, J.; Hough, W. L.; MacFarlane, D.; Rogers, R. D. *Chem. Commun.* **2011**, *47*, 2267−2269. (c) Mukherjee, A.; Desiraju, G. R. *Chem. Commun.* **2011**, *47*, 4090−4092. (d) Cinčić, D.; Friščić, T. F.; Jones, W. *J. Am. Chem. Soc.* **2008**, *130*, 7524−7525. (e) Childs, S. L.; Chyall, L. J.; Dunlap, J. T.; Smolenskaya, V. N.; Stahly, B. C.; Stahly, G. P. *J. Am. Chem. Soc.* **2004**, *126*, 13335−13342. (f) Remenar, J. F.; Morissette, S. L.; Peterson, M. L.; Moulton, B.; MacPhee, J. M.; Guzmán, H. R.; Almarsson, O. *J. Am. Chem. Soc.* **2003**, *125*, 8456−8457.

(4) (a) Friščić, T.; Trask, A. V.; Jones, W.; Motherwell, W. D. S. *Angew. Chem., Int. Ed.* **2006**, *45*, 7546−7550. (b) Trask, A. V.; Motherwell, W. D. S.; Jones, W. *Cryst. Growth Des.* **2005**, *5*, 1013−1021. (c) Sun, C. C.; Hou, H. *Cryst. Growth. Des.* **2008**, *8*, 1575−1579. (d) Bučar, D.-K.; Henry, R. F.; Lou, X.; Duerst, R. W.; MacGillivray, L. R.; Zhang, G. G. Z. *Cryst. Growth Des.* **2009**, *9*, 1932−1943. (e) Bučar, D.-K.; Henry, R. F.; Lou, X.; Borchardt, T. B.; Zhang, G. G. Z. *Chem. Commun.* **2007**, 525−527.

(5) (a) Florence, A. J.; Johnston, A.; Price, S. L.; Nowell, H.; Kennedy, A. R.; Shankland, N. *J. Pharm. Sci.* **2006**, *95*, 1918−1930. (b) Florence, A. J.; Leech, C. K.; Shankland, N.; Shankland, K.; Johnston, A. *CrystEngComm* **2006**, *8*, 746−747. (c) Porter, W. W., III; Elie, S. G.; Matzger, A J. *Cryst. Growth Des.* **2008**, *8*, 14−16. (d) Habgood, M.; Deij, M. A.; Mazurek, J.; Price, S. L.; ter Horst, J. H. *Cryst. Growth Des.* **2010**, *10*, 903−910.

(6) Meanwell, N. A. *Annu. Rep. Med. Chem.* **2008**, *43*, 373−404.
(7) (a) Goud, N. R.; Babu, N. J.; Nangia, A. *Cryst. Growth Des.* **2011**, *11*, 1930−1939. (b) Brondel, N.; Moynihan, E. J. A.; Lehane, K. N.; Eccles, K. S.; Elcoate, C. J.; Coles, S. J.; Lawrence, S. E.; Maguire, A. R. *CrystEngComm* **2010**, *12*, 2910−2927. (c) Eccles, K. S.; Elcoate, C. J.; Stokes, S. P.; Maguire, A. R.; Lawrence, S. E. *Cryst. Growth Des.* **2010**, *10*, 4243−4245. (d) Eccles, K. S.; Elcoate, C. J.; Maguire, A. R.; Lawrence, S. E. *Cryst. Growth Des.* **2011**, *11*, 4433−4439.
(8) Haynes, D. A.; Chisholm, J. A.; Jones, W.; Motherwell, W. D. S. *CrystEngComm* **2004**, *6*, 584−588.
(9) (a) Adsmond, D. A.; Grant, D. J. *J. Pharm. Sci.* **2001**, *90*, 2058−2077. (b) Perlovich, G. L.; Ryzhakov, A. M.; Tkachev, V. V.; Hansen, L. K. *Cryst. Growth Des.* **2010**, *11*, 1067−1081.
(10) (a) Caira, M. R. *Mol. Pharmaceutics* **2007**, *4*, 310−316. (b) Ghosh, S.; Bag, P. P.; Reddy, C. M. *Cryst. Growth Des.* **2011**, *11*, 3489−3503.
(11) (a) McIntosh, J. M.; Robinson, R. H. M.; Selbie, F. R.; Reidy, J. P.; Elliott Blake, H.; Guttman, L. *Lancet* **1945**, *246*, 97−99. (b) Jawetz, E. Sulfonamides and Trimethoprim. In *Basic & Clinical Pharmacology*, 2nd ed.; Katzung, B. G., Ed.; Lange Medical Publications: Los Altos, CA, 1984; pp 554−558.
(12) (a) Khan, M.; Enkelmann, V.; Brunkalus, G. *J. Am. Chem. Soc.* **2010**, *132*, 5254−5263. (b) Vishweshwar, P.; McMahon, J. A.; Bis, J. A.; Zaworotko, M. J. *J. Pharm. Sci.* **2006**, *3*, 499−516. (c) Jones, W.; Motherwell, W. D. S.; Trask, A. V. *MRS Bull.* **2006**, *31*, 875−879. (d) Shan, N.; Zaworotko, M. J. *Drug Discovery Today* **2008**, *13*, 440−446. (e) Aakeröy, C. B.; Forbes, S.; Desper, J. *J. Am. Chem. Soc.* **2009**, *131*, 17048−17049.
(13) (a) Joshi, V. V.; Tiwari, R. K.; Patel, T. C.; Singh, T. P. *Indian J. Phys., A.* **1983**, *57A*, 79−89. (b) Shin, H. S.; Ihn, G. S.; Kim, H. S.; Koo, C. H. *J. Korean Chem. Soc.* **1974**, *18*, 329−340.
(14) (a) Sarma, B.; Thakuria, R.; Nath, N. K.; Nangia, A. *CrystEngComm* **2011**, *13*, 3232−3240. (b) Nangia, A. *Cryst. Eng.* **2001**, *4*, 49−59. (c) Vishweshwar, P.; Nangia, A.; Lynch, V. M. *Cryst. Growth Des.* **2003**, *3*, 783−790. (d) Almarsson, Ö.; Zaworotko, M. J. *Chem. Commun.* **2004**, 1889−1896. (e) Desiraju, G. R. *J. Chem. Sci* **2010**, *122*, 667−675.
(15) Bučar, D.-K.; Henry, R. F.; Lou, X.; Duerst, R. W.; Borchardt, T. B.; MacGillivray, L. R.; Zhang, G. G. Z. *Mol. Pharmaceutics* **2007**, *4*, 339−346.
(16) Zhang, G. G. Z.; Henry, R. F.; Borchardt, T. B.; Lou, X. *J. Pharm. Sci.* **2007**, *96*, 990−995.
(17) (a) Childs, S. L.; Stahly, G. P.; Park, A. *Mol. Pharmaceutics* **2007**, *4*, 323−338. (b) Bhogala, B. R.; Basavoju, B. R.; Nangia, A. *CrystEngComm* **2005**, *7*, 551−562. (c) Mohamed, S.; Tocher, D. A.; Vickers, M.; Karamertzanis, P. G.; Price, S. L. *Cryst. Growth Des.* **2009**, *9*, 2881−2889.
(18) (a) Etter, M. C.; MacDonald, J. C.; Bernstein, J. *Acta Crystallogr.* **1990**, *B46*, 256−262. (b) Bernstein, J.; Davis, R. E.; Shimoni, L.; Chang, N.-L. *Angew. Chem., Int. Ed.* **1995**, *34*, 1555−1573.
(19) Bis, J. A.; Zaworotko, M. J. *Cryst. Growth Des.* **2005**, *5*, 1169−1179.
(20) Cruz-Cabeza, A. J.; Groom, C. R. *CrystEngComm* **2011**, *13*, 93−98.
(21) (a) Katritzky, A. R.; Hall, C. D.; El-Gendy, B. E.-D. M.; Draghici, B. *J. Comput.-Aided Mol. Des.* **2010**, *24*, 475−484. (b) Martin, Y. C. *J. Comput.-Aided Mol. Des.* **2010**, *23*, 693−704.
(22) Coe, B. J.; Harries, J. L.; Harris, J. A.; Brunschwig, B. S.; Coles, S. J.; Light, M. E.; Hursthouse, M. B. *Dalton Trans.* **2004**, *18*, 2935−2942.
(23) *SaintPlus*; Bruker AXS Inc.: Madison, WI, USA, 1999.
(24) Hooft, R. W. W. Nonius BV, Delft, The Netherlands, 1998.
(25) Otwinowski, Z.; Minor, W. In *Methods in Enzymology*, Eds.; Carter Jr., C. W.; Sweet, R. M., 1997; Vol. *276* (*Macromolecular Crystallography, Part A*), pp 307−326.
(26) Sheldrick, G. M. *Acta Crystallogr.* **2008**, *A64*, 112−122.
(27) Bruno, I. J.; Cole, J. C.; Edgington, P. R.; Kessler, M.; Macrae, C. F. *Acta Crystallogr.* **2002**, *B58*, 389−397.
(28) (a) Infantes, L.; Fábián, L.; Motherwell, W. D. S. *CrystEngComm* **2007**, *9*, 65−71. (b) Cruz-Cabeza, A. J.; Pidcock, E.; Day, G. M.; Motherwell, W. D. S.; Jones, W. *CrystEngComm* **2007**, *9*, 556−560. (c) Wood, P. A.; Borwick, S. J.; Watkin, D. J.; Motherwell, W. D. S.; Allen, F. H. *Acta Crystallogr.* **2008**, *B64*, 393−396.
(29) The reported inclusion complex of sulfamethazine and *β*-cyclodextrin (refcode: LILLUN) was excluded, since the compounds of interest were organic co-crystals, salts, or solvates. In addition, the reported complex of sulfamethazine and trimethoprim (refcode: SMZTMP) was excluded since the complex was incorrectly characterized as a co-crystal.
(30) (a) Fleischman, S. G.; Kuduva, S. S.; McMahon, J. A.; Moulton, B.; Bailey Walsh, R. D.; Rodríguez-Hornedo, N.; Zaworotko, M. J. *Cryst. Growth Des.* **2003**, *3*, 909−919. (b) Childs, S. L.; Rodríguez-Hornedo, N.; Reddy, L. S.; Jayasankar, A.; Maheshwari, C.; McCausland, L.; Shipplett, R.; Stahly, B. C. *CrystEngComm* **2008**, *10*, 856−864.
(31) pK_a values were calculated using a single point calculation in SPARC pK_a calculator (http://sparc.chem.uga.edu/sparc/).
(32) CCDC refcodes: IRILUQ, HEKRUK, IRILOK, IRIMEB, IRIMEB01, QASHAX, XIFKUT, SMZTMP01, SORWIF, YOSMOI, RASSUZ, VIGVOW, YIZQAA, COVXIU, SACCAF, QASHAB, RIWLOY, YIDJIE, XOBCOH, HADNAB, SORWEB, VUGMIT, DAHNIJ, GEYSAE, GEYSAE01, HADMOO, PVVAWG01, VUGMOZ, XEXCAE, XEXCEI, SABDOQ, AWIJEW, EXAMUM, EXANAT, EXANEX, EXANIB, EXANOH, EXANUN, EXAPEZ, EXAPID, EXAPID01, EXAPUP.
(33) (a) Rebek, J., Jr.; Askew, B.; Killoran, M.; Nemeth, D.; Lin, F.-T. *J. Am. Chem. Soc.* **1987**, *109*, 2426−2431. (b) Rebek, J., Jr.; Nemeth, D. *J. Am. Chem. Soc.* **1986**, *108*, 5637−5638. (c) Sessler, J. L.; Lawrence, C. M.; Jayawickramarajah, J. *Chem. Soc. Rev.* **2007**, *36*, 314−325.
(34) Aakeröy, C. B.; Rajbanshi, A.; Li, Z. J.; Desper, J. *CrystEngComm* **2010**, *12*, 4231−4239.
(35) Chen, I.-J.; MacKerell, A. D., Jr. *Theor. Chem. Acc.* **2000**, *103*, 483−494.
(36) Childs, S. L.; Hardcastle, K. I. *CrystEngComm* **2007**, *9*, 364−367.
(37) (a) Etter, M. C. *Acc. Chem. Res.* **1990**, *23*, 120−126. (b) Childs, S. L.; Wood, P. A.; Rodríguez-Hornedo, N.; Reddy, L. S.; Hardcastle, K. I. *Cryst. Growth Des.* **2009**, *9*, 1869−1888.
(38) Selected examples: (a) Weyna, D. R.; Shattock, T.; Vishweshwar, P.; Zaworotko, M. J. *Cryst. Growth Des.* **2009**, *9*, 1106−1123. (b) Oswald, I. D. H.; Motherwell, W. D. S.; Parsons, S. *Acta Crystallogr.* **2005**, *B61*, 46−57. (c) Zhang, Z.-H.; Tan, X.; Chen, S.-C. *Acta Crystallogr.* **2009**, *C65*, 457−459. (d) Oswald, I. D. H.; Allan, D. R.; McGregor, P. A.; Motherwell, W. D. S.; Parsons, S.; Pulham, C. R. *Acta Crystallogr.* **2002**, *B58*, 1057−1066.
(39) CCDC refcodes: AGOYOK, AGOYOK01, AMIDIJ, BOQDOA, COZKUL, DUCSAW, ITIQIL, MOYLOC, MOYMAP, MUPQAP, QAMRUS, VUJTAW, YUCQUJ, XUYJUX, XUYKIM, EPUQEM.
(40) Remko, M. *J. Phys. Chem. A* **2003**, *107*, 720−725.
(41) Bettinetti, G.; Caira, M. R.; Callegari, A.; Merli, M.; Sorrenti, M.; Tadini, C. *J. Pharm. Sci.* **2000**, *89*, 478−489.
(42) Nakai, H.; Takasuka, M.; Shiro, M. *J. Chem. Soc., Perkin Trans. II* **1984**, 1459−1464.
(43) Caira, M. R.; Bettinetti, G.; Sorrenti, M.; Catenacci, L. *J. Pharm. Sci.* **2003**, *92*, 2164−2176.
(44) Guiseppetti, G.; Tadini, C.; Bettinetti, G. *Acta Crystallogr.* **1994**, *C50*, 1289−1291.
(45) Lu, J.; Cruz-Cabeza, A. J.; Rohani, S.; Jennings, M. C. *Acta Crystallogr.* **2011**, *C67*, 306−309.
(46) Bettinetti, G.; Sardone, N. *Acta Crystallogr.* **1997**, *C53*, 594−597.
(47) Lynch, D. E.; Sandhu, P.; Parsons, S. *Aust. J. Chem.* **2000**, *53*, 383−387.
(48) Caira, M. R. *J. Crystallogr. Spectrosc. Res.* **1992**, *22*, 193−200.
(49) Caira, M. R. *J. Crystallogr. Spectrosc. Res.* **1991**, *5*, 641−648.
(50) Luccaciu, R.; Ionescu, C.; Wildervanck, A.; Caira, M. R. *X-Ray Struct. Anal. Online* **2008**, *24*, x87−x88.
(51) Caira, M. R. *J. Chem. Crystallogr.* **1994**, *24*, 695−701.

(52) Varma, A. K.; Tiwari, R. K. *J. T. R. Chem.* **1999**, *6*, 13−21.
(53) Caira, M. R.; Mohamed, R. *Acta Crystallogr.* **1993**, *B49*, 760−768.
(54) Coles, S. J.; Hursthouse, M. B.; Mayer, T. A.; Threlfall, T. L.; 2000, University of Southampton, Crystal Structure Report Archive. (doi:http://dx.doi.org/10.3737/ecrystals.chem.soton.ac.uk/196).
(55) Caira, M. R.; Mohamed, R. *Supramol. Chem.* **1993**, *2*, 201−207.
(56) Rambaud, J.; Maury, L.; Pauvert, B.; Audran, M.; Lasserre, Y.; Berge, G.; Declercq, J.-P. *Acta Crystallogr.* **1985**, *C41*, 133−134.
(57) Sardone, N.; Bettinetti, G.; Sorrenti, M. *Acta Crystallogr.* **1997**, *C53*, 1295−1299.
(58) Deutsch, H. M.; VanDerveer, D. G.; Zalkow, L. H. *Acta Crystallogr.* **1985**, *C41*, 1116−1118.
(59) Patel, U.; Haridas, M.; Singh, T. P. *Acta Crystallogr.* **1988**, *C44*, 1264−1267.
(60) Leger, J. M.; Alberola, S.; Carpy, A. *Acta Crystallogr.* **1977**, *B33*, 1455−1459.
(61) Caira, M. R.; Nassimbeni, L. R.; Wildervanck, A. F. *J. Chem. Soc., Perkin Trans. 2* **1995**, 2213−2216.
(62) Lu, E.; Rodríguez-Hornedo, N.; Suryanarayanan, R. *CrystEngComm* **2008**, *10*, 665−668.
(63) Ghosh, M.; Basak, A. K.; Mazumdar, S. K.; Sheldrik, B. *Acta Crystallogr.* **1991**, *C47*, 577−580.
(64) Wong, M. W.; Leung-Toung, R.; Wentrup, C. *J. Am. Chem. Soc.* **1993**, *115*, 2465−2472.
(65) Amidine and imidine tautomers of SMT modeled using Spartan '10 (Wave function, Inc., Irvine, CA) software. Dipole moments and electrostatic potential maps obtained from equilibrium geometry of each tautomer using AM1 calculations.
(66) Arijit, M.; Grobelny, P.; Thakur, T. S.; Desiraju, G. R. *Cryst. Growth Des.* **2011**, *11*, 2637−2653.
(67) Hristova, Y. R.; Smulders, M. M. J.; Clegg, J. K.; Breiner, B.; Nitschke, J. R. *Chem. Sci.* **2011**, *2*, 638−641.